Author for correspondence:
George Em Karniadakis
e-mail: george_karniadakis@brown.edu

†Present address: Department of Ocean and Mechanical Engineering, Florida Atlantic University, Boca Raton, FL 33431, USA.

THE ROYAL SOCIETY
PUBLISHING

Patient-specific blood rheology in sickle-cell anaemia

Xuejin Li[1], E. Du[2,†], Huan Lei[3], Yu-Hang Tang[1], Ming Dao[2], Subra Suresh[4,5] and George Em Karniadakis[1]

[1]Division of Applied Mathematics, Brown University, Providence, RI 02912, USA
[2]Department of Materials Science and Engineering, Massachusetts Institute of Technology, Cambridge, MA 02139, USA
[3]Computational Sciences and Mathematics Division, Pacific Northwest National Laboratory, Richland, WA 99354, USA
[4]Department of Biomedical Engineering, and [5]Department of Materials Science and Engineering, Carnegie Mellon University, Pittsburgh, PA 15213, USA

Sickle-cell anaemia (SCA) is an inherited blood disorder exhibiting heterogeneous cell morphology and abnormal rheology, especially under hypoxic conditions. By using a multiscale red blood cell (RBC) model with parameters derived from patient-specific data, we present a mesoscopic computational study of the haemodynamic and rheological characteristics of blood from SCA patients with hydroxyurea (HU) treatment (on-HU) and those without HU treatment (off-HU). We determine the shear viscosity of blood in health as well as in different states of disease. Our results suggest that treatment with HU improves or worsens the rheological characteristics of blood in SCA depending on the degree of hypoxia. However, on-HU groups always have higher levels of haematocrit-to-viscosity ratio (HVR) than off-HU groups, indicating that HU can indeed improve the oxygen transport potential of blood. Our patient-specific computational simulations suggest that the HVR level, rather than the shear viscosity of sickle RBC suspensions, may be a more reliable indicator in assessing the response to HU treatment.

1. Introduction

Blood is a non-Newtonian fluid that delivers nutrients and oxygen to living cells and removes their waste products. The viscosity of blood is a direct measure of the ability of blood to flow through the vessels. It is generally believed that five factors, namely, haematocrit (Hct), red blood cell (RBC) deformability, RBC aggregation, plasma viscosity and temperature, primarily determine the haemodynamic and rheological behaviour of blood [1].

SCA is an inherited blood disorder exhibiting abnormal rheology and haemodynamics under hypoxic conditions [2,3]. In SCA, mechanically fragile and poorly deformable RBCs contribute to impaired blood flow and other pathophysiological aspects of the disease. In addition, sickle RBC suspensions exhibit different levels of viscosity for different cell morphologies, which are dependent on the rate of deoxygenation (DeOxy) [4,5]. Gradual DeOxy is known to result in predominantly elongated- and classic sickle-shaped RBCs, which are intrinsically more rigid and viscous. The increase in blood viscosity is much greater when DeOxy is rapid (resulting in less distorted but highly viscous granular-shaped RBCs) than when it is gradual. When the flow of blood is relatively slow, cellular reactions that lead to adhesions of sickle RBCs to vascular endothelium can take place, resulting in vaso-occlusion and consequent clinical manifestations such as organ damage, pain and even death.

A change in blood rheological properties is usually linked to haematological diseases and, therefore, the viscosity of blood has long been used as an indicator for understanding the implications and treatment routes of this type of diseases. Although many experimental studies have been devoted to the measurement of sickle blood viscosity, considerable uncertainty exists with respect to the effect of hydroxyurea (HU) treatment [6–8] on the viscosity of

sickle blood: it has been reported that the viscosity may increase [9], decrease [10] or even remains unchanged [11] for patients with SCA after treated with HU. For example, in a case reported by Fattori *et al.* [9], they observed an increase in blood viscosity in their patient treated with HU for SCA. They also found a significant increase in haematocrit in this patient. However, in another case reported by Lemonne *et al.* [11], they observed that blood viscosity did not increase but remained as before in HU-treated patients. They also found that haematocrit did not significantly increase in their patients. Thus, the effect of HU treatment to blood viscosity in SCA cannot be attributed to just one factor, it is better understood as a multi-factorial process that involves Hct, cell volume and deformability, etc. Actually, two effects appear to counteract each other: on the one hand, HU treatment is associated with an elevated mean corpuscular volume (MCV) and an increased Hct, resulting in a higher blood viscosity [9]. On the other hand, HU treatment is also associated with improved cell hydration [12] and cell deformability [13,14], and consequently a lower blood viscosity [10]. Interestingly, sickle RBCs after HU treatment always exhibit higher RBC deformability and higher MCV, which raises the question: To what extent does the HU treatment enhance RBC performance in microcirculation, thereby improving oxygen delivery in the body?

Computational modelling and simulations of blood flow in microcapillaries have improved considerably in recent years [15–20]. For example, a multiscale RBC (MS-RBC) model [21,22] has been employed to quantify the adhesive and dynamic properties of sickle RBC suspensions in tube flows [23,24]. Available evidence indicates that adhesive interaction between sickle RBCs and vascular endothelium plays a key role in triggering vaso-occlusion phenomenon. Despite these findings, many important aspects of rheological and flow properties of sickle blood, especially of the HU effect on the complex and abnormal rheological behaviour of sickle RBCs and sickle blood, are still poorly understood. It is known that the origin of SCA can be traced to a common molecular basis, but individual patients with SCA have a highly variable clinical phenotype. For these reasons, there is a compelling need to develop a unique predictive *patient-specific* model of SCA to quantify the collective dynamics and rheology of blood flow in SCA. Such a model would provide a more reliable method and an overall modelling framework to extract rheological properties of blood flow in SCA from a variety of independent experimental methods. In this paper, we present a computational simulation framework for assessing implications of SCA from *patient-based* information and for extracting *quantitative* prediction of rheological properties of sickle blood through which clinical inventions could potentially be designed and evaluated more effectively.

2. Material and methods

2.1. Selection of sickle blood samples

Blood samples from four patients with SCA were collected in ethylenediaminetetraacetic acid and stored at 4°C for *in vitro* testing within 3 days of blood withdrawal. The four samples included two with HU treatment (on-HU) and two without HU treatment (off-HU). Table 1 shows selected haematologic and haemorheologic parameters in these four samples from SCA patients.

Table 1. Selected haematologic parameters from four SCA patients. The symbols MCHC and MCV in the table denote mean corpuscular haemoglobin concentration and mean corpuscular volume, respectively. S-P-I and S-P-II represent two samples of SCA patients not treated with HU, whereas S-P-III and S-P-IV represent the other two samples from SCA patients treated with HU.

	off-HU		on-HU	
	S-P-I	S-P-II	S-P-III	S-P-IV
Hct (%)	22.9	18.6	21.9	29.2
MCV (fl)	83.0	83.3	99.1	99.0
MCHC (g dl^{-1})	36.7	36.6	35.6	34.2
HbS (%)	84.2	90.1	72.4	86.0
HbF (%)	11.9	6.0	24.1	10.0
HbA (%)	0.0	0.0	0.0	0.0
HbA$_2$ (%)	3.9	3.9	3.5	4.0

Table 2. Values of cell density and MCHC in different cell fractions.

cell fraction	I	II	III	IV
cell density (g ml^{-1})	1.081	1.091	1.100	1.111
MCHC (g dl^{-1})	27.3	30.9	34.9	50.0

Each blood sample, 1 ml in volume, was washed twice with phosphate-buffered saline (PBS) at a centrifuge frequency of 2000 r.p.m. for 5 min at 21°C and fractionated into four density sub-populations using an Optiprep-based gradient medium. The estimated mean corpuscular haemoglobin concentration (MCHC) values of the four density subpopulations were 27.3, 30.9, 34.9 and 50.0 g dl^{-1} (table 2). Each fractionated density was suspended in RPMI-1640 medium containing 1% w/v bovine serum albumin (BSA) for *in vitro* sickling measurement using a polydimethylsiloxane (PDMS)-based microfluidic hypoxia assay, which provided measurements of cell sickling under controlled oxygen concentration conditions at 37°C, including a fully oxygenation (Oxy) state (20% O$_2$), a short-term hypoxia (40 s) and a long-term hypoxia (4 min). For the two hypoxic conditions, O$_2$ concentration dropped from 20% to less than 5% within 15 s and maintained at 2% for the rest period of time.

Cell sickling was identified visually by changes in cell shape and cell texture associated with DeOxy on a Zeiss Axiovert 200 (Zeiss, Thornwood, NY, USA) inverted microscope with a 414/46 nm band-pass filter. The morphology of sickled and unsickled cells was categorized into four major groups, including discoid- (D), granular- (G), elongated- (E) and classic sickle-shaped (S) RBCs.

2.2. Simulation model and method

We studied the shear viscosity of sickle blood with the help of the MS-RBC model based on the dissipative particle dynamics (DPD) simulation technique [25]. For completeness, the method and the model are briefly reviewed below; more comprehensive details are available elsewhere [21,22].

2.2.1. The dissipative particle dynamics method

The DPD method is a stochastic simulation technique that describes a set of particles moving together in a Lagrangian fashion (i.e. a method where the motion of particles is observed

in a moving reference frame) subject to simplified pairwise conservative, dissipative and random forces [25]. In DPD simulation, particles represent a cluster of molecules, rather than single atoms and their position and momentum are updated in continuous phase but spaced at discrete time steps [26]. A common choice of the soft repulsion for the DPD particles permits us to use larger integration time steps than usually allowed by the molecular dynamics (MD) simulation technique. As a result, DPD is a simple but intrinsically more adaptable simulation method for modelling the dynamic and rheological properties of simple and complex fluids, such as blood flow.

2.2.2. Red blood cell models

In the MS-RBC model, the cell membrane is modelled by a two-dimensional triangulated network with N_v vertices, where each vertex is represented by a DPD particle. The vertices are connected by N_s viscoelastic bonds so as to impose proper membrane mechanics. Specifically, the elastic part of bond is represented by

$$V_s = \sum_{j \in 1 \ldots N_s} \left[\frac{k_B T l_m (3x_j^2 - 2x_j^3)}{4p(1 - x_j)} + \frac{k_p}{(n-1)l_j^{n-1}} \right], \qquad (2.1)$$

where l_j is the length of the spring j, l_m is the maximum spring extension, $x_j = l_j/l_m$, p is the persistence length, $k_B T$ is the energy unit, k_p is the spring constant and n is a specified exponent. The membrane viscosity is imposed by introducing a viscous force on each spring. The bending resistance of the RBC membrane is modelled by

$$V_b = \sum_{j \in 1 \ldots N_s} k_b [1 - \cos(\theta_j - \theta_0)], \qquad (2.2)$$

where k_b is the bending constant, θ_j is the instantaneous angle between two adjacent triangles having the common edge j and θ_0 is the spontaneous angle. Constraints on the area and volume conservation of RBC are imposed to mimic the area-preserving lipid bilayer and the incompressible interior fluid. The corresponding energy is given by

$$V_{a+v} = \sum_{j \in 1 \ldots N_t} \frac{k_d (A_j - A_0)^2}{2A_0} + \frac{k_a (A - A_0^{tot})^2}{2A_0^{tot}} + \frac{k_v (V - V_0^{tot})^2}{2V_0^{tot}}, \qquad (2.3)$$

where N_t is the number of triangles in the membrane network, A_0 is the triangle area, and k_d, k_a and k_v are the local area, global area and volume constraint coefficients, respectively. The terms A_0^{tot} and V_0^{tot} are the specified total area and volume, respectively.

The RBC membrane interacts with the fluid particles through DPD forces, and the temperature of the system is controlled through the DPD thermostat. The internal and external fluids are modelled by collections of free DPD particles and their separation is enforced by bounce-back reflections of these particles at the RBC membrane surface. The model has been validated in a number of studies including the simulations of healthy [27], malaria-infected [28] and SCA RBC flow conditions [24]. The sickle RBC model is constructed by applying surface tension on an MS-RBC membrane, representing the distortion of the cell membrane due to the polymerization of HbS molecules and alignment of fibres inside the RBC. The distorted shape is redefined as the equilibrium state of the sickle RBC with minimum free energy. Detailed description of the sickle RBC model can be found in [23,29].

2.2.3. Aggregation model

The aggregation interaction between RBCs plays a major role in rheological property of blood [27]. In this study, the intercellular aggregation interaction is approximated using the Morse potential

$$U_r^M = D_e [e^{2\beta(r_0 - r)} - 2e^{\beta(r_0 - r)}], \qquad (2.4)$$

where D_e is the well depth of the Morse potential, and β characterizes the interaction range. For the MS-RBC model, the Morse potential interactions are implemented between every pair of vertices of separate RBCs if they lie within a defined potential cutoff radius [27].

2.3. Rheological prediction

Blood viscosity was computed from simulations of a suspension of RBCs in plane Couette flow (see the electronic supplementary material, video clip). As the sickle RBCs are more rigid and less flexible, in many clinical case reports blood viscosity are usually determined at lower shear rates less than, say $225\,\mathrm{s}^{-1}$. For this reason, the shear rates are tested only in the range of $0-160\,\mathrm{s}^{-1}$. On average, the shear rate and particle number density in simulations were verified to be spatially uniform over time, and the viscosities were computed as functions of the shear rate over the above range.

3. Results and discussion

The abnormal rheological properties of sickle RBCs are correlated with the significantly lowered cell deformability. In the sickle RBCs, their equivalent shear modulus is significantly higher than that for the healthy RBC [14,30,31]. In this study, we modelled a healthy RBC using the MS-RBC model with the following parameters: $N_v = 500$; RBC area $A_0 = 135.2\,\mu\mathrm{m}^2$ and volume $V_0 = 92.4\,\mu\mathrm{m}^3$; RBC membrane bending modulus $k_{c,0} = 2.4 \times 10^{-19}\,\mathrm{J}$; shear modulus $\mu_0 = 6.3\,\mathrm{pN}\,\mu\mathrm{m}^{-1}$. Following Lei & Karniadakis [23], the effective shear modulus of the sickle RBC was first chosen to be 2000 times larger than the value of the healthy RBC in the current study. Recent studies suggest that RBC aggregation properties are likely to be involved in the pathophysiology of SCA [32], and the force required to disrupt aggregates of RBCs in case of SCA is around four times greater than that in the healthy RBC [33]. The RBC aggregation interactions are modelled by the Morse potential with the following properties [24,27]: $\beta = 1.5$, $r_0 = 0.3$ and the well depth of the Morse potential is set at $D_{e,0} = 3.0$ for the healthy RBC and $D_e = 12.0$ for the sickle RBC.

In the model system, the domain dimensions are set to $40.0 \times 40.0 \times 28.0\,\mu\mathrm{m}$. The number of RBCs depends on the Hct level and cell volume for each blood sample. For example, there are approximately 194 RBCs in the simulation box at Hct = 40% and MCV = $92.4\,\mu\mathrm{m}^3$. The equations of motion are integrated using a modified velocity-Verlet algorithm with $\lambda = 0.50$ and time step $\Delta t = 0.001\tau$. Typical simulation takes about 5.0×10^6 time steps to compute the required statistics.

With the parameters defined as shown above, we first consider the healthy blood. The measured shear viscosity with respect to shear rate is plotted in figure 1a. We find that the simulation results can be fitted by $\eta = be^{-a/\dot{\gamma}^{0.5}} + c$, where a, b and c are fitting parameters specified in the figure. The numerical results show that the healthy blood behaves as a non-Newtonian fluid under normal conditions, i.e. the shear viscosity decreases with the increasing of shear rate, which are in agreement with the experimental results [34]. We then examined the shear viscosity of sickle blood at 40% Hct with three distinct types of sickle RBCs—the granular-, elongated- and classic sickle-shaped types—reported in previous experiments [4]. Our results show that the abnormal rheological properties of sickle RBCs are correlated with the cell morphology, and the sickle RBC suspensions
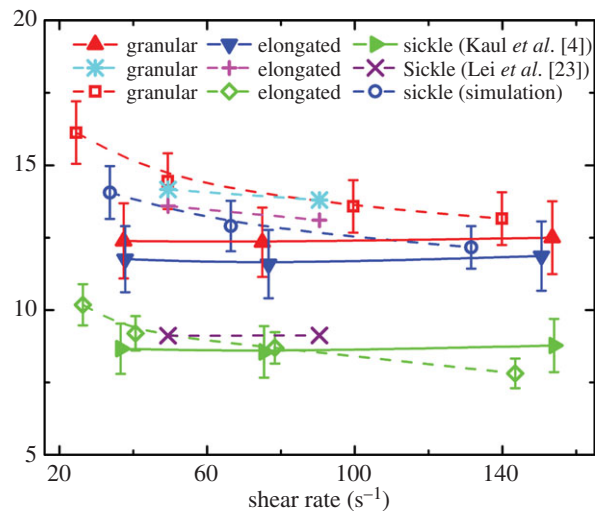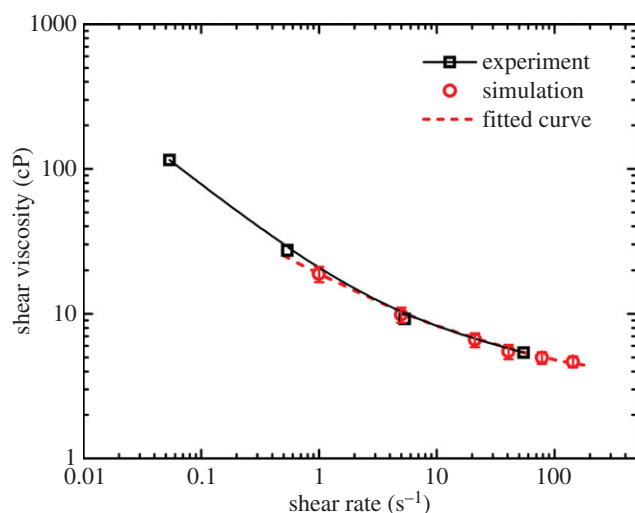
Figure 1. (a) Shear viscosity of healthy blood at Hct = 45% and (b) sickle RBC suspensions at Hct = 40% with different cell morphology. For comparison, the experimental measured shear viscosity of whole blood in health at Hct = 45% by Chien et al. [34] and in SCA at Hct = 40% by Kaul et al. [4], and previous computational simulations of sickle RBC suspensions at Hct = 40% by Lei et al. [23] are shown in these figures. The dashed line in panel (a) represents the fitted curve to the simulation result by $\eta = b e^{-a/\dot{\gamma}^{0.5}} + c$, where $\dot{\gamma}$ is the shear rate; a, b and c are 6.6×10^{-3}, -2374.7 and 2378.0, respectively. (Online version in colour.)

exhibit different viscosity values for different cell shapes: the granular-shaped RBC suspension is the most viscous, while the classic sickle-shaped RBC suspension has a lower viscosity. However, the shear viscosity of sickle RBC suspensions containing elongated RBCs shows a dramatic decrease. The numerical results agree with available experimental data [4] and numerical simulations [23]. Figure 1b summarizes these findings. The error bars in the figure show the statistical error of a set of calculated viscosity values, by increasing or decreasing the default value of shear modulus μ_0 by 10%.

The sickle RBCs has decreased deformability, causing abnormal rheology in sickle blood and eventually various complications of SCA. To verify the significant role of cell deformability in determining the rheological property of individual sickle RBCs, we performed numerical simulations of sickle RBCs in shear flow at different shear modulus values. Here, we adopted the granular-shaped RBCs as an example. In figure 2, we show the simulation results. We found that the viscosity of sickle RBC suspension increases with increasing effective shear modulus. It becomes weakly dependent on shear rate when the normalized shear modulus (i.e. the ratio of shear modulus of the sickle RBC to that of the healthy RBC) reaches about 1000.

We then carried out numerical simulations of *patient-based* samples to predict the shear viscosity of blood in SCA by incorporating clinical data of SCA patients. Parameters related to these data, including biophysical characteristics, haematologic and haemorheologic parameters in SCA patients are summarized in table 1. In these data, the level of HbS was found to be the highest in the off-HU/S-P-II group (90.1%), moderate in the off-HU/S-P-I group (84.2%) and the on-HU/S-P-IV (86.0%) group and the lowest in the on-HU/S-P-III group (72.4%). By contrast, the highest level of HbF was seen in the on-HU/S-P-III group (24.1%), moderate in the on-HU/S-P-IV (10.0%) group and the off-HU/S-P-I group (11.9%), and lowest in the off-HU/S-P-II group (6.0%). One possible reason for these different HbS/HbF levels is the variability in the clinical symptoms of different SCA patients: some patients have
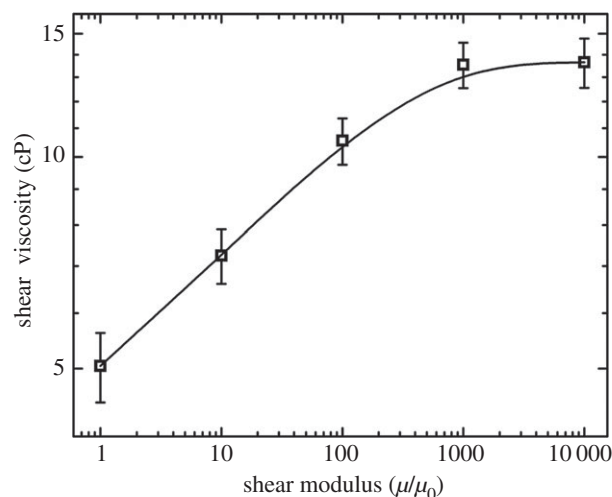

Figure 2. Functional dependence of shear viscosity of sickle RBC suspensions on the normalized shear modulus obtained from DPD simulations.

mild symptoms, while others are frequently hospitalized for more serious complications. When the values of MCV were compared between the off-HU and on-HU groups, it was found that the MCV values are always higher in the on-HU groups than those in the off-HU groups. This is consistent with previous observations that sickle RBCs after treatment with HU always exhibit higher MCV values. We studied the rheological properties of blood in SCA using these specific clinical data for individual patients at three different states: (i) fully Oxy state, (ii) short-term DeOxy state and (iii) long-term DeOxy state.

Similar to the study of Kaul et al. [35], sickle blood is separated into four major fractions (I–IV) according to the cell density (see figure 3). Selected characteristics and morphologic analysis of SCA patients are summarized in table 3. One major subpopulation consists of sickle RBCs with a density similar to that of healthy RBCs (fraction II, SS2), the other subpopulation is very dense (fraction IV, SS4) and contains mainly irreversible sickle cells (ISCs). The sickle RBCs lighter than fraction II contain a high subpopulation of reticulocytes (fraction I, SS1) [35], while fraction III (SS3) denotes a group
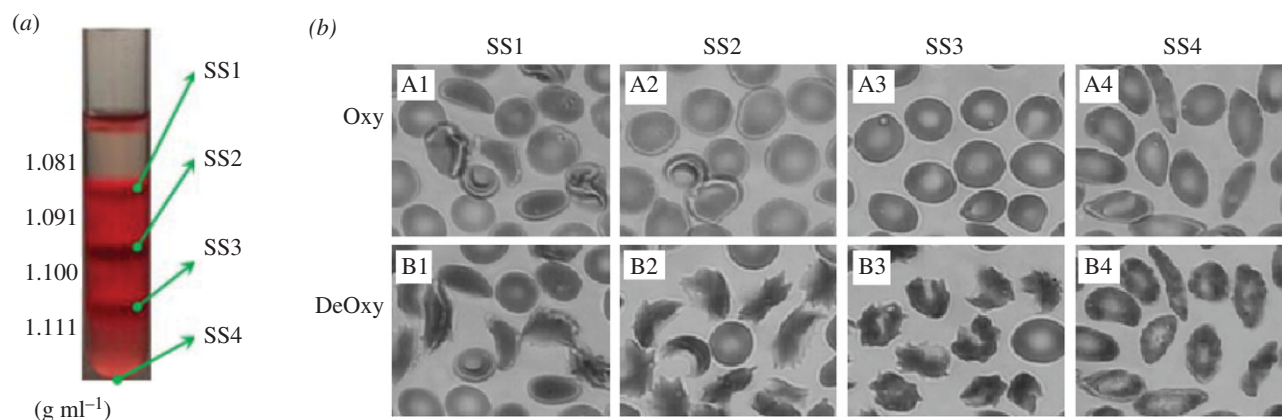
Figure 3. (*a*) sickle RBCs separated by different cell densities. Sickle blood is separated into four major cell subpopulations (fractions I–IV, SS1–SS4). (*b*) Typical shapes of sickle RBCs at each subpopulation under Oxy and DeOxy states. A1–A4 show sickle RBCs in fractions SS1–SS4 under Oxy state respectively; most cells have a discoid morphology. B1–B4 show sickle RBCs in fractions SS1-SS4 under DeOxy state respectively; a large percentage of cells appear to be granular and classic sickle morphology. (Online version in colour.)

Table 3. General characteristics and morphologic analysis of sickle RBCs in four representative SCA patients. Symbols D, G, E and S indicate discoid-, granular-, elongated- and classic sickle-shaped RBCs, respectively.

condition		sample	sickling (%)	fraction	sickled cells (%)				deformable cells (%)			
					D	G	E	S	D	G	E	S
Oxy	Off-HU	S-P-I	0.0	SS1	—	—	—	—	3.5	0.4	2.4	—
				SS2	—	—	—	—	43.4	2.6	4.3	1.8
				SS3	—	—	—	—	20.6	0.9	9.2	1.3
				SS4	—	—	—	—	1.4	0.7	6.7	0.8
		S-P-II	0.0	SS1	—	—	—	—	3.4	2.7	—	—
				SS2	—	—	—	—	37.7	2.4	4.9	—
				SS3	—	—	—	—	15.0	1.1	5.2	—
				SS4	—	—	—	—	5.6	—	18.1	3.9
	on-HU	S-P-III	0.0	SS1	—	—	—	—	16.0	0.9	1.9	0.6
				SS2	—	—	—	—	38.7	1.6	9.5	—
				SS3	—	—	—	—	17.3	2.2	6.1	0.7
				SS4	—	—	—	—	2.5	0.9	1.1	—
		S-P-IV	0.0	SS1	—	—	—	—	2.5	0.6	—	—
				SS2	—	—	—	—	28.8	1.9	—	—
				SS3	—	—	—	—	55.6	3.8	—	—
				SS4	—	—	—	—	3.1	2.5	0.6	0.6
short-term DeOxy (40 s)	Off-HU	S-P-I	20.2	SS1	—	—	—	—	2.6	0.5	3.0	—
				SS2	—	4.4	—	—	38.2	2.4	5.7	1.6
				SS3	—	5.8	1.8	—	14.7	1.6	7.8	0.4
				SS4	—	2.5	5.1	0.6	1.3	—	—	—
		S-P-II	39.0	SS1	—	—	—	—	2.8	1.7	1.6	—
				SS2	—	—	—	—	36.8	4.7	3.5	—
				SS3	—	12.5	—	0.3	5.4	0.5	2.7	—
				SS4	0.6	12.5	5.9	7.2	—	—	1.3	—
	On-HU	S-P-III	9.4	SS1	—	—	—	—	18.0	1.0	—	0.4
				SS2	—	3.1	—	—	38.4	—	7.5	0.8
				SS3	—	4.4	—	—	15.8	—	6.3	—
				SS4	—	1.4	0.5	—	1.6	—	0.8	—

Table 3. (*Continued.*)

condition	sample	sickling (%)	fraction	sickled cells (%)				deformable cells (%)			
				D	G	E	S	D	G	E	S
	S-P-IV	3.1	SS1	—	—	—	—	3.1	1.3	—	0.6
			SS2	—	—	—	—	47.5	1.9	—	—
			SS3	—	2.5	—	—	33.8	1.9	3.1	0.6
			SS4	—	—	—	0.6	2.5	—	0.6	
long-term DeOxy (4 *min*)	Off-HU	S-P-I	59.5	SS1	—	—	—	—	2.6	0.9	2.6	0.8
			SS2	—	21.5	—	5.0	18.6	2.1	4.3	0.7
			SS3	—	18.1	—	5.9	5.3	1.3	0.9	0.4
			SS4	—	3.4	4.3	1.3	—	—	—	—
		S-P-II	80.4	SS1	—	—	0.7	0.9	2.2	0.9	1.2	—
			SS2	—	17.4	—	15.4	9.2	1.9	1.0	0.5
			SS3	—	18.5	0.3	—	1.8	0.5	0.4	—
			SS4	1.3	9.6	6.9	9.4	—	—	—	—
	On-HU	S-P-III	34.4	SS1	—	1.3	—	2.0	10.9	1.3	3.9	—
			SS2	—	4.6	—	2.8	31.2	—	10.9	0.8
			SS3	—	16.6	—	3.9	3.6	—	1.4	0.9
			SS4	—	2.0	1.2	—	1.0	—	—	—
		S-P-IV	57.6	SS1	—	—	—	—	2.5	0.6	—	—
			SS2	—	7.5	—	7.5	15.6	—	—	—
			SS3	—	31.3	—	4.4	23.7	—	—	—
			SS4	—	5.0	1.9	—	—	—	—	—

distinctly located between fractions II and IV. It is known that sickle RBCs exhibit various morphological characteristics and different cell rigidity depending on cell density and DeOxy procedure [31,36]. Previous studies have clearly shown that the deformability of individual sickle RBCs is decreased even under fully Oxy state [30,31] when compared with healthy RBCs. It deteriorates further with reductions in oxygen concentration [36]: upon DeOxy, the equivalent shear modulus of sickle RBCs is increased by 100–1000-fold (i.e. the deformability decreases very significantly) concomitantly with cell morphological changes [31]. Taking all these facts into consideration, different effective shear modulus values emerge for sickle RBCs in different cell density subpopulations under Oxy and DeOxy. Under Oxy, based on the experimental measured shear modulus data by Evans *et al.* [30], the effective shear modulus is set to $\mu = 1.0\mu_0$, $1.2\mu_0$, $1.5\mu_0$ and $3.0\mu_0$ for RBCs in fractions I, II, III and IV, respectively. Under DeOxy, we considered four distinct types of sickle RBCs with different membrane properties under shear flow based our previous simulations [23,24]: for an SS1 deformable cell with a low MCHC value, we set the effective shear modulus $\mu = (5-10)\mu_0$. For an SS2 cell with a moderate MCHC value, the effective shear modulus is one or two orders of magnitude greater than the value of healthy RBCs, so we set $\mu = (50-100)\mu_0$. For an ISC of the SS4 type, in which the effective shear modulus is increased by at least two or three orders of magnitude compared with that of healthy RBCs [31], we set $\mu = (1000-2000)\mu_0$. For a rigid discocyte cell of SS3 type with a higher MCHC value, we set $\mu = (250-500)\mu_0$ for the comparative study. In

addition, for the deformable RBCs in each cell fraction, we assume that these RBCs have a similar deformability with the ones in the same cell fraction under Oxy.

As shown in table 1, patients with SCA have Hct values that are roughly half of the normal value (e.g. about 18.6–21.9% compared to about 40–45% normally). It is known that haematocrit is the most obvious determinant of blood viscosity [37]. A decrease in haematocrit leads to a decrease in blood viscosity. Moreover, the whole blood viscosity also depends on RBC deformability, which is considered the second most important determinant of blood viscosity. Blood containing sickle RBCs is more viscous than normal blood, because the sickle RBCs are more rigid and their membranes are stiffer. HU treatment improves cell deformability but also increases cell volume (see the MCV values in table 1). The joint influence of HU on RBC structural and mechanical properties may significantly affect the blood flow in SCA patients. In order to develop a quantitative assessment of the efficacy of HU treatment on blood viscosity, we examined how sickle RBC suspensions moved in shear flow. Specifically, we computed and compared the blood viscosity at different shear rates among normal blood, on-HU and off-HU groups exposed to different oxygen tensions. The values of shear viscosity of sickle blood obtained from the DPD simulations are shown in figure 4. We analyse the simulation results at these three different states:

(1) *Under Oxy state.* The average shear viscosity of sickle blood is found to be significantly less than that of normal blood at all three shear rates (i.e. $\dot\gamma = 40$, 80 and
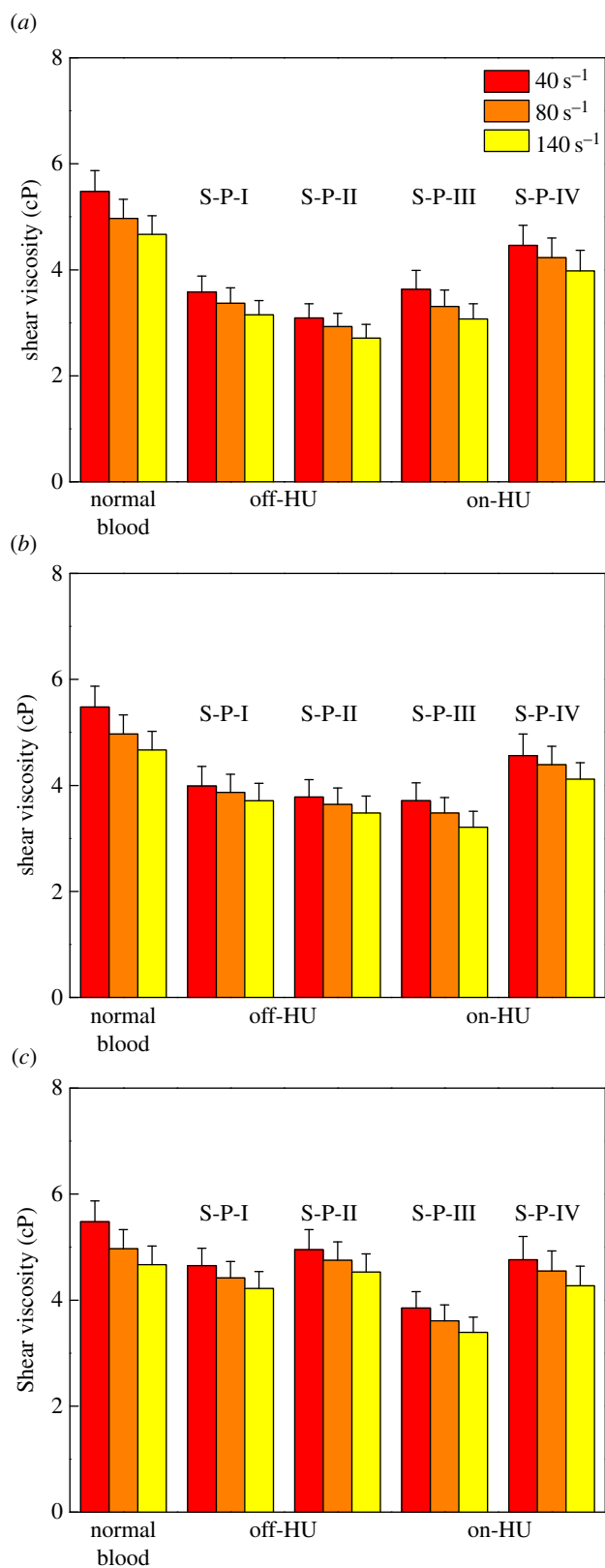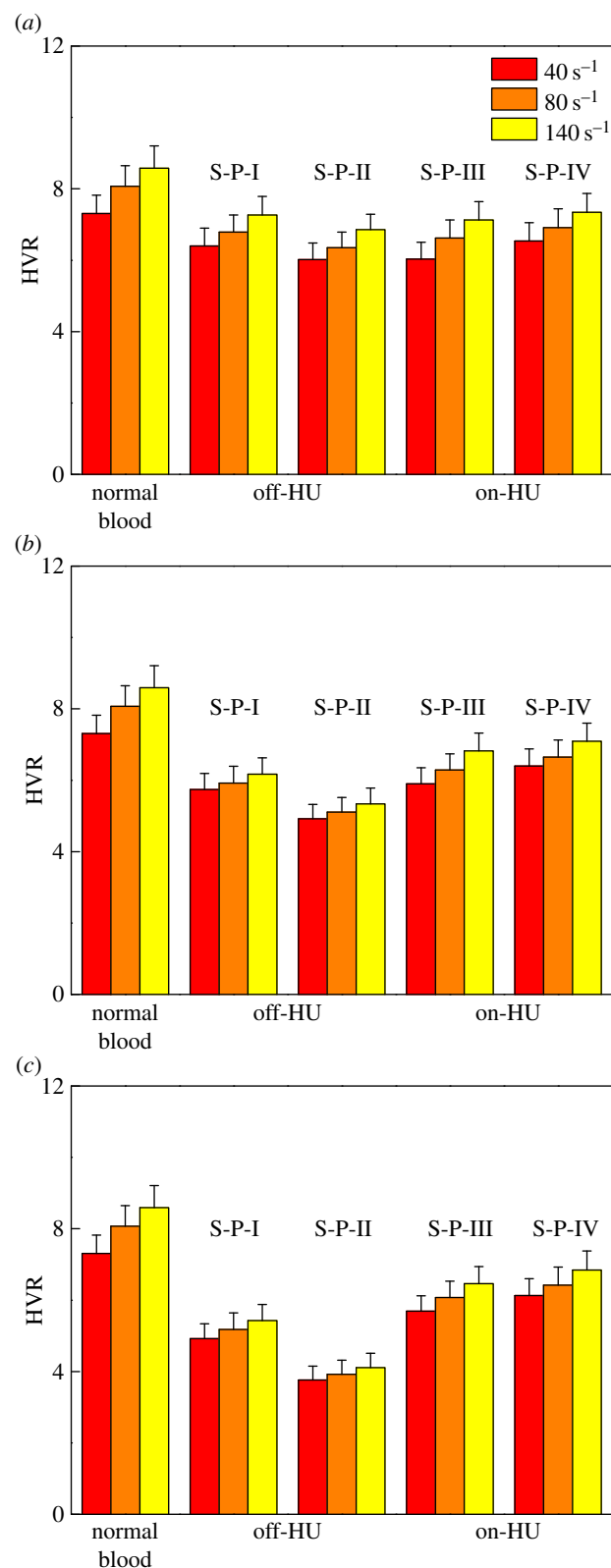
Figure 4. Predicted shear viscosity of blood in SCA at fully Oxy state (*a*), short-term DeOxy state (*b*) and long-term DeOxy state (*c*). The dark grey, grey and light grey columns show the viscosity values at shear rate $\dot{\gamma} = 40.0$, 80.0 and 140.0 s^{-1}, respectively. (Online version in colour.)

Figure 5. Predicted HVR values of blood in SCA at fully Oxy state (*a*), short-term DeOxy state (*b*) and long-term DeOxy state (*c*). The dark grey, grey and light grey columns show the viscosity values at shear rate $\dot{\gamma} = 40.0$, 80.0 and 140.0 s^{-1}, respectively. (Online version in colour.)

140 s^{-1}), and the off-HU/S-P-II group has the lowest viscosity. It is known that haematocrit is a primary determinant in blood shear viscosity under this specific condition. The lower shear viscosity of sickle blood samples is mainly associated with the reduced Hct values than those of normal control.

(2) *Under short-term DeOxy state.* After 40 s of DeOxy, the viscosity of sickle blood increases, and the difference between the on-HU groups and the off-HU groups becomes smaller. Moreover, the on-HU/S-P-III group yields a slightly lower viscosity than the off-HU/S-P-I group. The on-HU/S-P-IV group still yields the highest blood viscosity among the four sickle blood samples.

This is mainly due to its higher Hct value than the other three sickle blood samples. The altered blood viscosity in SCA cases is also associated with an increased number of sickle RBCs, especially the granular-shaped RBCs. For example, in the off-HU/S-P-I group and the off-HU/S-P-II group, there are 12.7% and 25.0% of RBCs becoming granular-shaped RBCs, respectively. It is known that the granular-shaped RBC suspensions are the most viscous. As a result, these changes bring an increase in sickle blood viscosity. In the off-HU/S-P-II group, more RBCs become sickled than those in the off-HU/S-P-I group. Associated with this change is a remarkable increase in blood viscosity of the off-HU/S-P-II group compared to the off-HU/S-P-I group.

(3) *Under long-term DeOxy state.* With an increase in DeOxy time, the shear viscosity in individual sickle blood samples increases. The increases we observed in viscosity of sickle blood are likely caused primarily by changes in cell morphology. As shown in table 3, the changes in cell morphology are remarkable with more rigid granular-shaped RBCs: in the off-HU/S-P-I group, the granular-shaped RBCs increased from 12.7 to 43.0%; in the off-HU/S-P-II group, the granular-shaped RBCs increased from 25.0 to 45.5%. Within the on-HU groups, the amount of granular-shaped RBCs are changed from 8.9% and 2.5% to 24.5% and 43.8% for the on-HU/S-P-III group and the on-HU/S-P-IV group, respectively. As we have demonstrated earlier, the granular-shaped RBC suspensions are the most viscous, and thus, a relatively large increase in the percentage of granular-shaped RBCs can cause marked increase in blood viscosity. Our results thus suggest two major parameters that can affect the blood viscosity in SCA after DeOxy: the haematocrit and cell morphology.

As the viscosity of blood is a direct measure of the resistance of blood to flow, an increase in blood viscosity would be expected to result in retarded blood flow thereby causing reduced oxygen delivery. However, an increase in blood viscosity might not be associated with increased risk in SCA [38]. The haematocrit-to-viscosity ratio (HVR), which reflects the oxygen transport efficiency of blood [32], is calculated for each subject at different shear rates.

For each case, we find that the HVR level increases with the shear rate (figure 5). Also, for the on-HU groups, the HVR levels are higher than those for the off-HU groups. Under Oxy states, all sickle blood samples share a similar blood viscosity at the same shear rate, and HU treatment seems to have no obvious influence. However, under DeOxy states, the HVR values of the of-HU groups decrease significantly and they are of much lower levels than those values of the on-HU groups. The higher HVR levels found in the on-HU groups indicate that the haemorheological oxygen transport potential of blood seems to be preserved in these groups. Thus, although blood viscosity cannot easily be compared between the different sickle blood samples, the high HVR levels found in the on-HU groups indicate a comparable high oxygen transport potential of blood. Here we want to mention that the functional dependence of the shear viscosity on the shear rate is associated with the Coutte flow set-up (constant shear rate), which is not necessarily transferable to the *in vivo* scenario. In addition, the shear viscosity is examined from four blood samples including two on-HU groups and two off-HU groups. Thus, further work with more patients and quantitative comparison to selective experiments is required to confirm and emphasize the rheological aspects of SCA—this may be investigated more systematically in future studies.

4. Summary

In summary, this study provides a unique, *patient-based* simulation at the molecular level on the rheological behaviour of sickle blood. Our data suggest that although systemic blood viscosity is not a major factor involved in the pathophysiology of this complication, decreased RBC oxygen transport efficiency, i.e. low haematocrit/viscosity ratio, could play a critical role. This ensemble of results thus leads to the conclusion that HU treatment can indeed improve the blood flow in SCA. Understanding the shear viscosity and the HVR level of sickle blood is, therefore, essential to explore new treatment strategies.

References

1. Baskurt O, Meiselman H. 2003 Blood rheology and hemodynamics. *Semin. Thromb. Hemost.* **29**, 435–450. (doi:10.1055/s-2003-44551)

2. Chien S, Usami S, Bertles JF. 1970 Abnormal rheology of oxygenated blood in sickle cell anemia. *J. Clin. Invest.* **49**, 623–634. (doi:10.1172/JCI106273)

3. Usami S, Chien S, Scholtz PM, Bertles JF. 1975 Effect of deoxygenation on blood rheology in sickle cell disease. *Microvasc. Res.* **9**, 324–334.

4. Kaul DK, Xue H. 1987 Rate of deoxygenation and rheologic behavior of blood in sickle cell anemia. *Blood* **77**, 1353–1361.

5. Du E, Diez-Silva M, Kato GJ, Dao M, Suresh S. 2015 Kinetics of sickle cell biorheology and implications for painful vasoocclusive crisis. *Proc. Natl Acad. Sci. USA* **112**, 1422–1427. (doi:10.1073/pnas.1424111112)

6. Charache S *et al.* 1992 Hydroxyurea: effects on hemoglobin F production in patients with sickle cell anemia. *Blood* **79**, 2555–2565.

7. Ferster A *et al.* 2001 Five years of experience with hydroxyurea in children and young adults with

sickle cell disease. *Blood* **97**, 3628–3632. (doi:10.1182/blood.V97.11.3628)

8. Akinsheye I, Alsultan A, Solovieff N, Ngo D, Baldwin C, Sebastiani P, Chui D, Steinberg M. 2011 Fetal hemoglobin in sickle cell anemia. *Blood* **118**, 19–27. (doi:10.1182/blood-2011-03-325258)

9. Fattori A, de Souza R, Saad S, Costa F. 2005 Acute myocardial infarction in sickle cell disease: a possible complication of hydroxyurea treatment. *Hematol. J.* **5**, 589–590. (doi:10.1038/sj.thj.6200572)

10. Ware R. 2010 How I use hydroxyurea to treat young patients with sickle cell anemia. *Blood* **115**, 5300–5311. (doi:10.1182/blood-2009-04-146852)

11. Lemonne N et al. 2015 Hydroxyurea treatment does not increase blood viscosity and improves red blood cell rheology in sickle cell anemia. *Haematologica* **100**, e383–e386. (doi:10.3324/haematol.2015.130435)

12. Ballas SK, Dover GJ, Charache S. 1989 Effect of hydroxyurea on the rheological properties of sickle erythrocytes *in vivo*. *Am. J. Hematol.* **32**, 1044–1111. (doi:10.1002/ajh.2830320206)

13. Brando M, Fontes A, Barjas-Castro M, Barbosa L, Costa F, Cesar C, Saad S. 2003 Optical tweezers for measuring red blood cell elasticity: application to the study of drug response in sickle cell disease. *Eur. J. Haematol.* **70**, 207–211. (doi:10.1034/j.1600-0609.2003.00027.x)

14. Byun H, Hillman TR, Higgins JM, Diez-Silva M, Peng Z, Dao M, Suresh S, Park Y. 2012 Optical measurement of biomechanical properties of individual erythrocytes from a sickle cell patient. *Acta Biomater.* **8**, 4130–4138. (doi:10.1016/j.actbio.2012.07.011)

15. Noguchi H, Gompper G. 2005 Shape transitions of fluid vesicles and red blood cells in capillary flows. *Proc. Natl Acad. Sci. USA* **102**, 14 159–14 164. (doi:10.1073/pnas.0504243102)

16. McWhirter JL, Noguchi H, Gompper G. 2009 Flow-induced clustering and alignment of vesicles and red blood cells in microcapillaries. *Proc. Natl Acad. Sci. USA* **106**, 6039–6043. (doi:10.1073/pnas.0811484106)

17. Quinn DJ, Pivkin IV, Wong SK, Chiam K-H, Dao M, Karniadakis GE, Suresh S. 2011 Combined simulation and experimental study of large deformation of red blood cells in microfluidic systems. *Ann. Biomed. Eng.* **39**, 1041–1050.

18. Bow H, Pivkin IV, Diez-Silva M, Goldfless SJ, Dao M, Niles JC, Suresh S, Han J. 2011 A microfabricated deformability-based flow cytometer with application to malaria. *Lab Chip* **11**, 1065–1073. (doi:10.1039/c0lc00472c)

19. Li XJ, Vlahovska PV, Karniadakis GE. 2013 Continuum- and particle-based modeling of shapes and dynamics of red blood cells in health and disease. *Soft Matter* **9**, 28–37. (doi:10.1039/C2SM26891D)

20. Li XJ, Peng ZL, Lei H, Dao M, Karniadakis GE. 2014 Probing red blood cell mechanics, rheology and dynamics with a two-component multiscale model. *Phil. Trans. R. Soc. A* **372**, 20130389. (doi:10.1098/rsta.2013.0389)

21. Pivkin IV, Karniadakis GE. 2008 Accurate coarse-grained modeling of red blood cells. *Phys. Rev. Lett.* **101**, 118105. (doi:10.1103/PhysRevLett.101.118105)

22. Fedosov DA, Caswell B, Karniadakis GE. 2010 A multiscale red blood cell model with accurate mechanics, rheology, and dynamics. *Biophys. J.* **98**, 2215–2225. (doi:10.1016/j.bpj.2010.02.002)

23. Lei H, Karniadakis GE. 2012 Quantifying the rheological and hemodynamic characteristics of sickle cell anemia. *Biophys. J.* **102**, 185–194. (doi:10.1016/j.bpj.2011.12.006)

24. Lei H, Karniadakis G. 2013 Probing vasoocclusion phenomena in sickle cell anemia via mesoscopic simulations. *Proc. Natl Acad. Sci. USA* **110**, 11 326–11 330. (doi:10.1073/pnas.1221297110)

25. Hoogerbrugge PJ, Koelman JMVA. 1992 Simulating microscopic hydrodynamic phenomena with dissipative particle dynamics. *Europhys. Lett.* **19**, 155–160. (doi:10.1209/0295-5075/19/3/001)

26. Li XJ, Pivkin IV, Liang HJ, Karniadakis GE. 2009 Shape transformations of membrane vesicles from amphiphilic triblock copolymers: a dissipative particle dynamics simulation study. *Macromolecules* **42**, 3195–3200. (doi:10.1021/ma9000918)

27. Fedosov DA, Pan WX, Caswell B, Gompper G, Karniadakis GE. 2011 Predicting human blood viscosity in silico. *Proc. Natl Acad. Sci. USA* **108**, 11 772–11 776. (doi:10.1073/pnas.1101210108)

28. Fedosov DA, Caswell B, Suresh S, Karniadakis GE. 2011 Quantifying the biophysical characteristics of *plasmodium-falciparum*-parasitized red blood cells in microcirculation. *Proc. Natl Acad. Sci. USA* **108**, 35–39. (doi:10.1073/pnas.1009492108)

29. Li XJ, Caswell B, Karniadakis GE. 2012 Effect of chain chirality on the self-assembly of sickle hemoglobin. *Biophys. J.* **103**, 1130–1140. (doi:10.1016/j.bpj.2012.08.017)

30. Evans E, Mohandas N, Leung A. 1984 Static and dynamics rigidities of normal and sickle erythrocytes: major influence of cell hemoglobin concentration. *J. Clin. Invest.* **73**, 477–488. (doi:10.1172/JCI111234)

31. Itoh T, Chien S, Usami S. 1995 Effects of hemoglobin concentration on deformability of individual sickle cells after deoxygenation. *Blood* **85**, 2245–2253.

32. Tripette J et al. 2009 Red blood cell aggregation, aggregate strength and oxygen transport potential of blood are abnormal in both homozygous sickle cell anemia and sickle-hemoglobin C disease. *Haematol. Hematol. J.* **94**, 1060–1065. (doi:10.3324/haematol.2008.005371)

33. Lemonne N, Connes P, Romana M, Vent-Schmidt J, Bourhis V, Lamarre Y, Etienne-Julan M. 2012 Increased blood viscosity and red blood cell aggregation in a patient with sickle cell anemia and smoldering myeloma. *Amer. J. Haematol.* **87**, E129. (doi:10.1002/ajh.23312)

34. Chien S, Usami S, Taylor HM, Lundberg JL, Gregersen MI. 1966 Effects of hematocrit and plasma proteins on human blood rheology at low shear rates. *J. Appl. Physiol.* **21**, 81–87.

35. Kaul D, Fabry M, Windisch P, Baez S, Nagel R. 1983 Erythrocytes in sickle cell anemia are heterogeneous in their rheological and hemodynamic characteristics. *J. Clin. Invest.* **72**, 22–31. (doi:10.1172/JCI110960)

36. Itoh T, Chien S, Usami S. 1992 Deformability measurements on individual sickle cells using a new system with PO2, and temperature control. *Blood* **79**, 2141–2147.

37. Stuart J, Kenny MW. 1980 Blood rheology. *J. Clin. Pathol.* **3**, 417–429. (doi:10.1136/jcp.33.5.417)

38. Connes P et al. 2014 Haemolysis and abnormal haemorheology in sickle cell anaemia. *Br. J. Haematol.* **165**, 564–572. (doi:10.1111/bjh.12786)